Supporting Information

A study of perturbations in structure and elastic modulus of bone microconstituents using bimodal amplitude modulated-frequency modulated atomic force microscopy

Yao Sun,[a] *Lien Hong Vu,*[b] *Nicholas Chew,*[b] *Zudin Puthucheary,*[b,c] *Matthew E. Cove,*[b] *Kaiyang Zeng,*[a,*]

[a] Department of Mechanical Engineering, National University of Singapore, 9 Engineering Drive 1, 117576, Singapore.

[b] Department of Medicine, Yong Loo Lin School of Medicine, National University of Singapore, 1E Kent Ridge Road, NUHS Tower Block Level 10, Singapore 119228.

[c] Division of Critical Care, Institute of Sports and Exercise Health, University College London Hospitals, UK, and Centre for Human Health and Performance, University College London, UK.

Correspondence and requests for materials should be addressed to Prof. K.Y.Zeng. (E-mail: mpezk@nus.edu.sg).

Principles of AM-FM technique [1]

In AM-FM, the force gradient between AFM tip and sample (k_{ts}) is a function of the second mode contact resonance frequency shift (Δf_2) [2]

$$k_{ts} \approx 2k_2 \Delta f_2 / f_2^0 . \quad \text{(S1)}$$

Herein, k_2 and f_2^0 are the second mode elastic constant of the probe and the second mode free vibration resonance frequency. Assuming that the tip-sample contact satisfies the Hertz contact, the force gradient can be written as the function of the equivalent elastic modulus of the tip-sample system:

$$k_{ts} = 2a_c E^* . \quad \text{(S2)}$$

where a_c is the tip-sample contact radius and E^* denotes the equivalent elastic modulus of the tip-sample system. From the Equation (S1) and (S2), E^* can be derived as a linear function of Δf_2, with a constant coefficient C.

$$E^* = k_2 \Delta f_2 / a_c f_2^0 = C \Delta f_2 \quad \text{(S3)}$$

Since a_c is unknown, a standard reference material with a known elastic modulus is used to determine the elastic modulus of the sample. If the elastic modulus of chosen reference material is approximately the same with the sample, the a_c of tip-reference system and tip-sample system are treated to be equal. The constant coefficient C can be decided by conducting the same experiment with same parameters on the reference material and obtaining from tip-reference equivalent elastic modulus and tip-reference second mode contact resonance frequency shift.

For Hertz contact model, the tip-sample contact stiffness is the first derivative of the applied force to the resultant deformation:

$$k^* = \frac{\delta F_N}{\delta \delta} = \sqrt[3]{6E^{*2}RF_N} \,. \tag{S4}$$

Here, δ, F_N and R are the resultant deformation, applied force and tip radius respectively. By adopting the reference material, the relationship between the tip-sample contact stiffness and tip-sample equivalent elastic modulus can be known from Equation (S4)

$$E^*_{s-tip} = E^*_{ref-tip}\left(\frac{k^*_{s-tip}/k_c}{k^*_{ref-tip}/k_c}\right)^{3/2}, \tag{S5}$$

where E^*_{s-tip}, $E^*_{ref-tip}$, k^*_{s-tip}, $k^*_{ref-tip}$ and k_c are tip-sample equivalent elastic modulus, tip-reference material equivalent elastic modulus, tip-sample contact stiffness, tip-reference material contact stiffness and cantilever spring constant respectively. For Hertz contact model, E^* is the function of elastic modulus of tip M_t and the elastic modulus of the sample M_s:

$$E^* = \frac{1}{M_t} + \frac{1}{M_s} \tag{S6}$$

From Equations S5 and S6, M_s can be derived as:

$$M_s = \{[(k^*_{ref-tip}/k_c)/(k^*_{s-tip}/k_c)]^{3/2}/M_{ref} + [[(k^*_{ref-tip}/k_c)/(k^*_{s-tip}/k_c)]^{3/2} - 1]/M_t\}^{-1} \tag{S7}$$

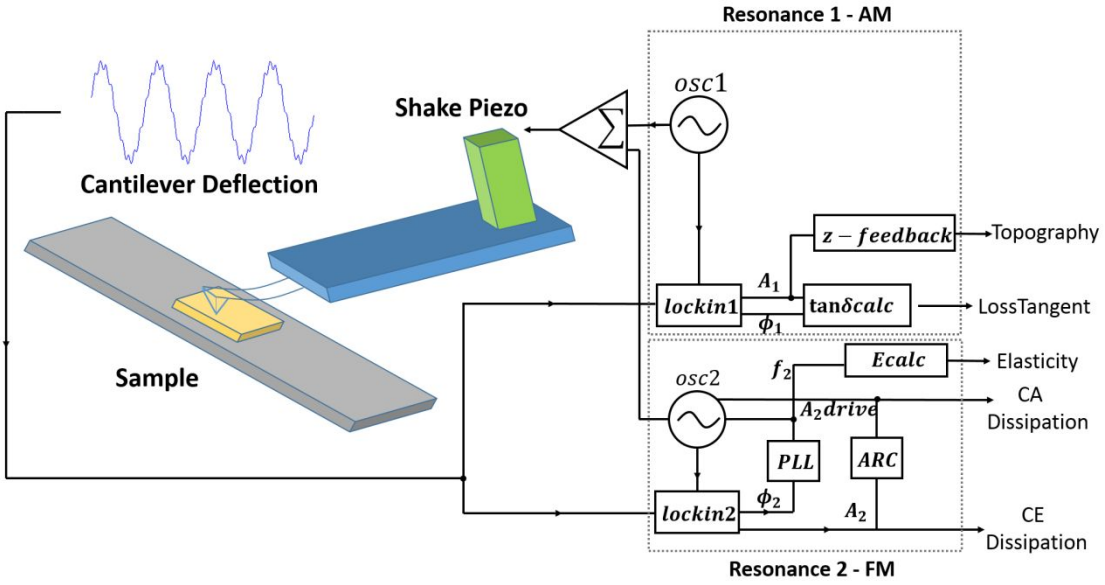

Figure S1. The schematic illustration of AM-FM technique [1].

Calculations of uncertainty and uncertainty propagation[3]

Quantifying uncertainties in measured properties of nanomaterials is necessary in AFM study. The dominant source of uncertainty is the nondimensional photodiode sensitivity (*m*) calibration rather than cantilever stiffness in our study since we scan the reference sample with same experimental parameters immediately after acquiring the stiffness image of bone sample. The Z-piezo sensitivity (C_Z) can be checked from the manufacture instruction note in our SPM system (MFP-3D, Asylum Research, Oxford Instruments, CA, USA). The C_Z is 72.4×10^{-9} m/V. The output of the data reduction equation (DRE) is the elastic modulus (E). The DRE for E has the form

$$E = f_1(\mathrm{Z}_{v,1},\ldots \mathrm{Z}_{v,\mathrm{n}},\delta_{v,1},\ldots\delta_{v,n},\mathrm{m}),$$

where $\mathrm{Z}_{v,\mathrm{i}}$ and $\delta_{v,\mathrm{i}}$ are the data points in the force-Z-piezo displacement (F-Z) curve. The core idea is that how is E changes if *m* changes a little. The photodiode sensitivity (C_L) can be determined by performing F-Z curves on pure silicon (Fig. S2a). For calibration, 40 F-Z curves are measured. The slope in the curves (V/nm) is determined by fitting a line to the upper half of the contact region. C_L is the inverse of this slope, which is approximately 6.74 nm/V. The *m* is 0.0931 with standard uncertainty 0.00261.

We adopt the Taylor series uncertainty method to provide uncertainty propagation. The Taylor series formula for the uncertainty in E is given as:

$$u_E^2 = (\frac{df_1}{dZ_{v1}}u_{z_{v1}})^2 + \ldots + (\frac{df_1}{dZ_{vn}}u_{z_{vn}})^2 + (\frac{df_1}{d\delta_{v1}}u_{\delta_{v1}})^2 + \ldots + (\frac{df_1}{d\delta_{vn}}u_{\delta_{vn}})^2 + (\frac{df_1}{dm}u_m)^2 .$$

The partial derivatives are evaluated numerically with the central difference method. The uncertainty and uncertainty propagation values we calculate from silicon are 4.58 GPa and 9.16 GPa with 95% confidence interval (CI). We replicate the whole process to calculate the uncertainty and uncertainty propagation of our bone samples. Fig. S2b shows one sample F-Z curve on mineral from the *sham* bone sample.

After fitting and Taylor expansion, the uncertainty and uncertainty propagation values of mineral from the *sham* bone are 25.13 GPa and 50.26 GPa with 95% CI. We conduct the F-Z measurements, uncertainty and uncertainty propagation calculations on collagen fibers and mineral from all the three bone groups (*sham*, *24 hour CLP* and *96 hour CLP*), we can obtain the whole sample uncertainty analysis table. We have added this uncertainty analysis table in the Supporting Information (Table S2).

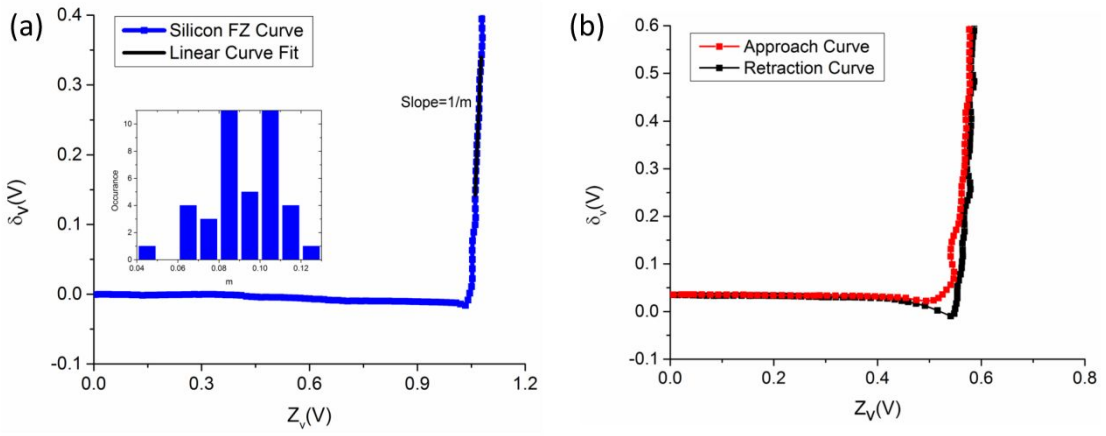

Figure S2. Force-displacement curves on (a) pure silicon wafer (These curves are used to calibrate the nondimensional photodiode sensitivity (*m*), which is defined as the inverse of the slope (volts/volts) of the deflection versus Z-piezo displacement curve in the repulsive regime of tip-sample interaction. There are totally 40 results for the fitting of *m*), and (b) the mineral from the *sham* bone sample.

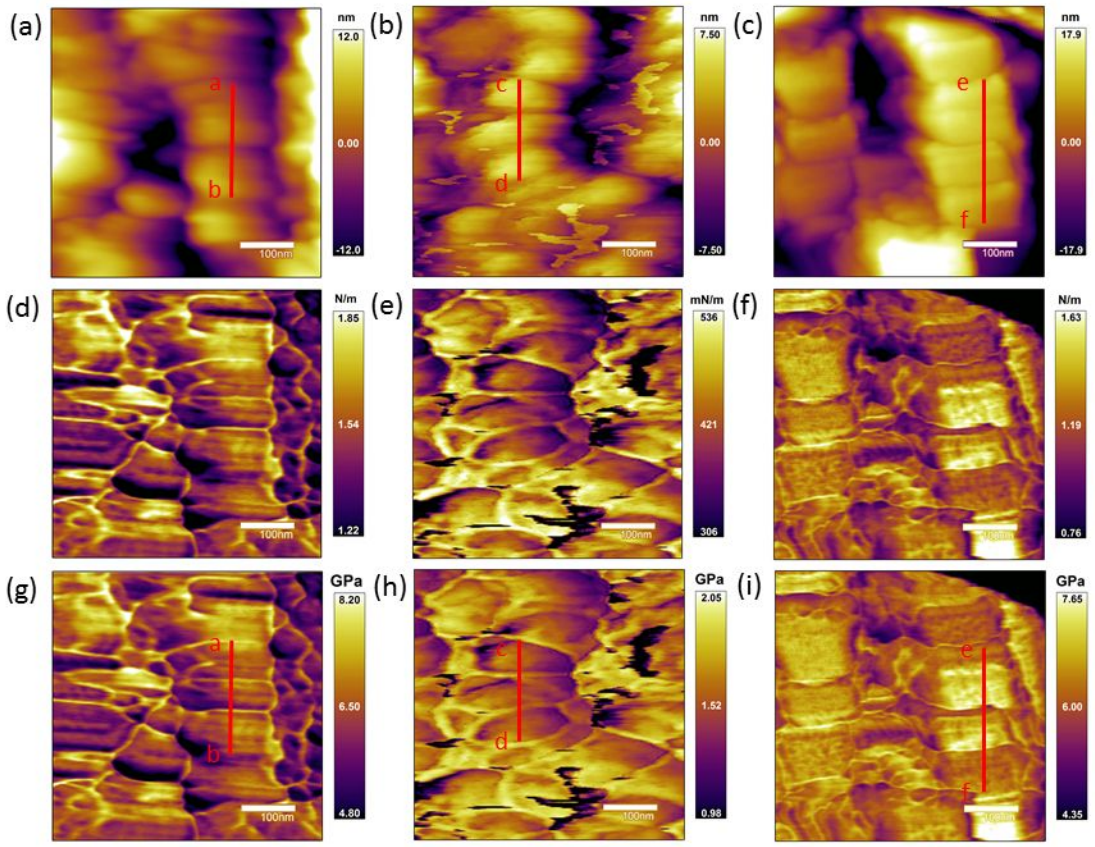

Figure S3. AM-FM images (500nm×500nm) of collagen fibers from the *sham* (1st column), *24 hour CLP* (2nd column) and *96 hour CLP* (3rd column) bone samples, respectively. (a) (b) (c) topography, (d) (e) (f) stiffness and (g) (h) (i) calculated elastic modulus images, respectively.

Calculations of Hamaker constant (*H*) and minimum distance of approach per cycle (d_{min}) of collagen fibers

For a sphere (tip)-plane (surface) interaction, there exists a well-known model:[4-6]

$$F_{ts} \approx -\frac{RH}{6d^2},$$

where R is the effective tip radius, d is the tip-surface distance and H is the Hamaker constant that accounts for the effects of vdW forces due to tip-surface chemistry. The tip we use is AC200TS (Asylum Research, Oxford Instruments, CA, USA) with 1st eigenmode spring constant 9.89nN/nm. The tip radius is provided by the manufacturer, $R \approx 10 \pm 1$ nm. We have employed $R \approx 10$ nm throughout the calculations. By fitting the force F_{ts} in the above equation to the F_{ts} versus distance profile, we can obtain the *H*. For example, by fitting the F_{ts} in the profile in Fig. S4 (black line), the *H* of collagen fibers from the *sham* bone sample can be derived. Linear aggression is carried out with the use of the standard lm function.

After the fitting the above profile, the *H* is 0.0312 atto *J* for collagen fibers from the *sham* bone sample. We adopt the average H value from 30 F_{ts} versus distance profiles. The average *H* of collagen fibers from the *sham* bone sample is 0.037 atto *J*. Similarly, we replicate the experiments on collagen fibers from the *24 hour CLP* and *96 hour CLP* bone samples. The *H* values of collagen fibers from the *24 hour CLP* and *96 hour CLP* bone samples are 0.173 atto *J* and 0.025 atto *J*.

After then, the $d_{\min}$ can be calculated from

$$H = -a[(\frac{d_{\min} + A_1}{A_1})^2 - 1]^{3/2},$$

where $a = \frac{3F_{D1}A_1^2}{R}\cos(\phi_1)$ and $F_{D1} = k_1 A_{01} / Q_1$, according to the published papers.[6-7]

Herein, $k_1, A_{01}, \mathrm{A}_1, Q_1$ are the 1st eigenmode spring constant, free amplitude, amplitude and Q factor. The parameters are k_1=9.89nN/nm, A_{01}=10.5 nm, A_1=7.48 nm, Q_1 =273.4. The calculated d_{min} are 0.15, 0.41 and 0.12 nm for collagen fibers from the *sham*, *24 hour CLP* and *96 hour CLP* bone samples. The d_{min} of collagen fibers from the *24 hour CLP* bone sample is larger than the those of collagen fibers from the *sham* and *96 hour CLP* bone samples, indicating the probable larger chemical heterogeneity of collagen fibers from the *24 hour CLP* bone sample. The true, or corrected height can be found by adding the d_{min} to the measured height value. Moreover, the corrected height image can be obtained by adding the d_{min} map to the measured one.

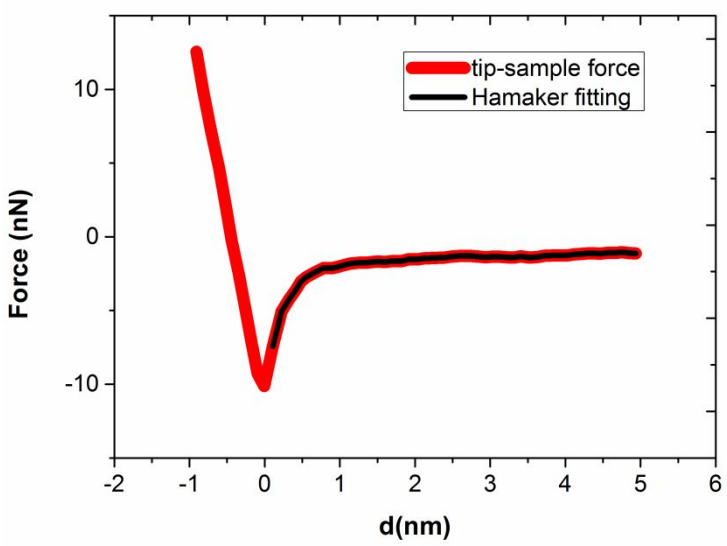

Figure S4. Representative force F_{ts} versus distance (d) profile for the collagen fibers from the *sham* bone sample.

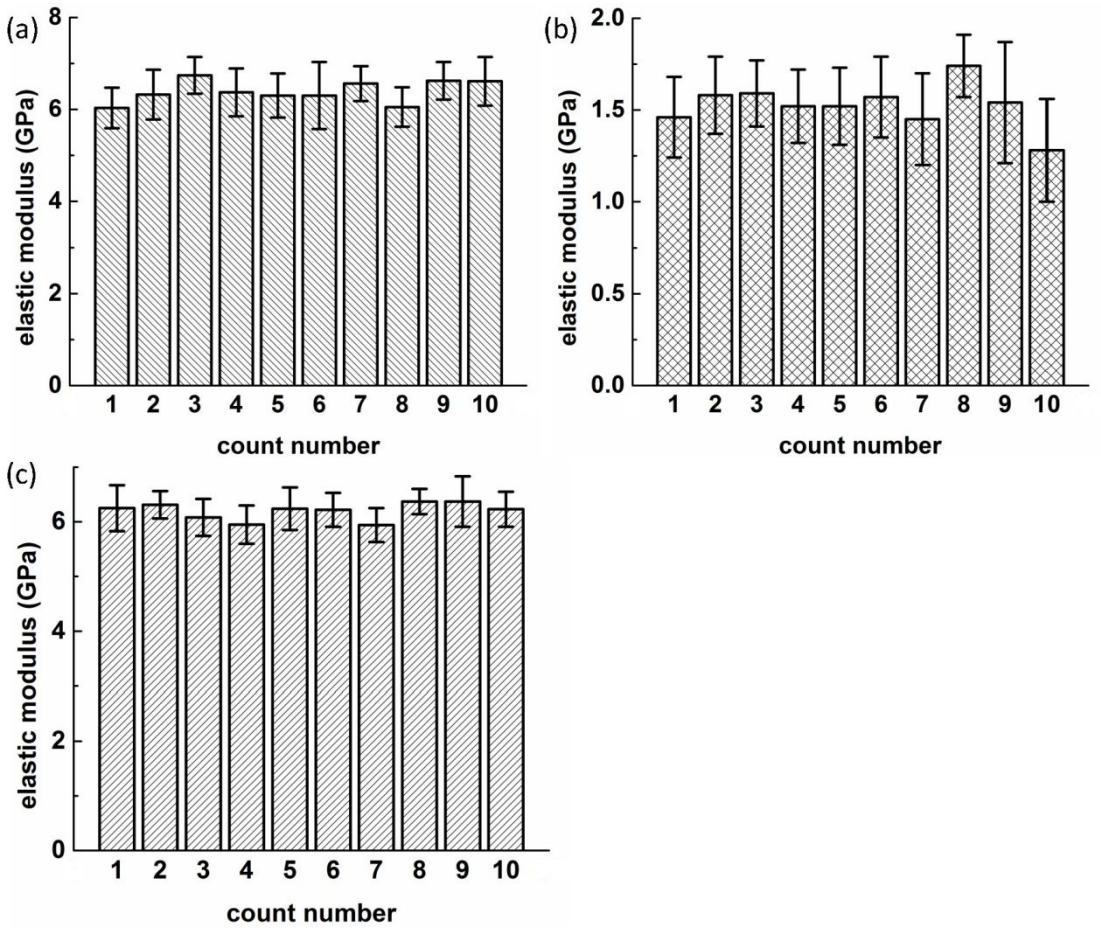

Figure S5. The elastic modulus charts of collagen fibers from ten (10) different (a) *sham*, (b) *24 hour CLP* and (c) *96 hour CLP* femur samples, respectively.

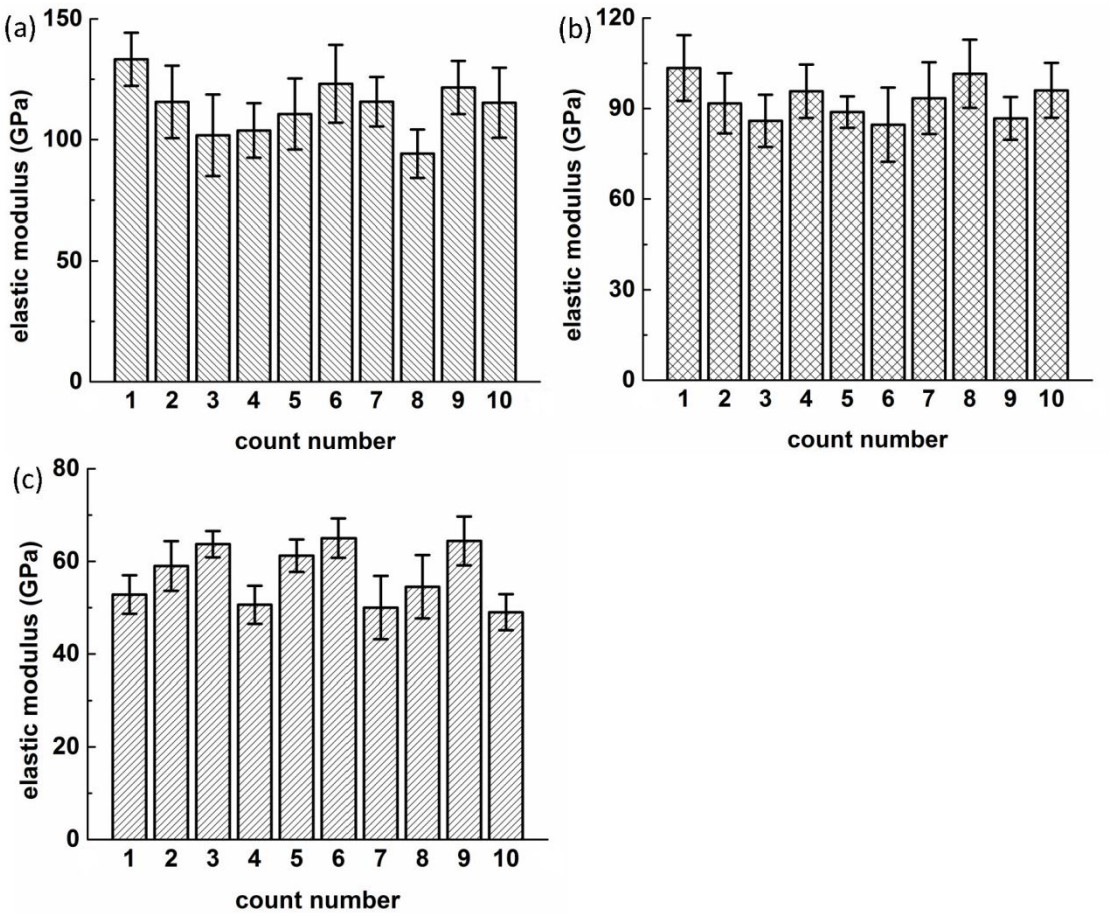

Figure S6. The elastic modulus charts of mineral from ten (10) different (a) *sham*, (b) *24 hour CLP* and (c) *96 hour CLP* femur samples, respectively.

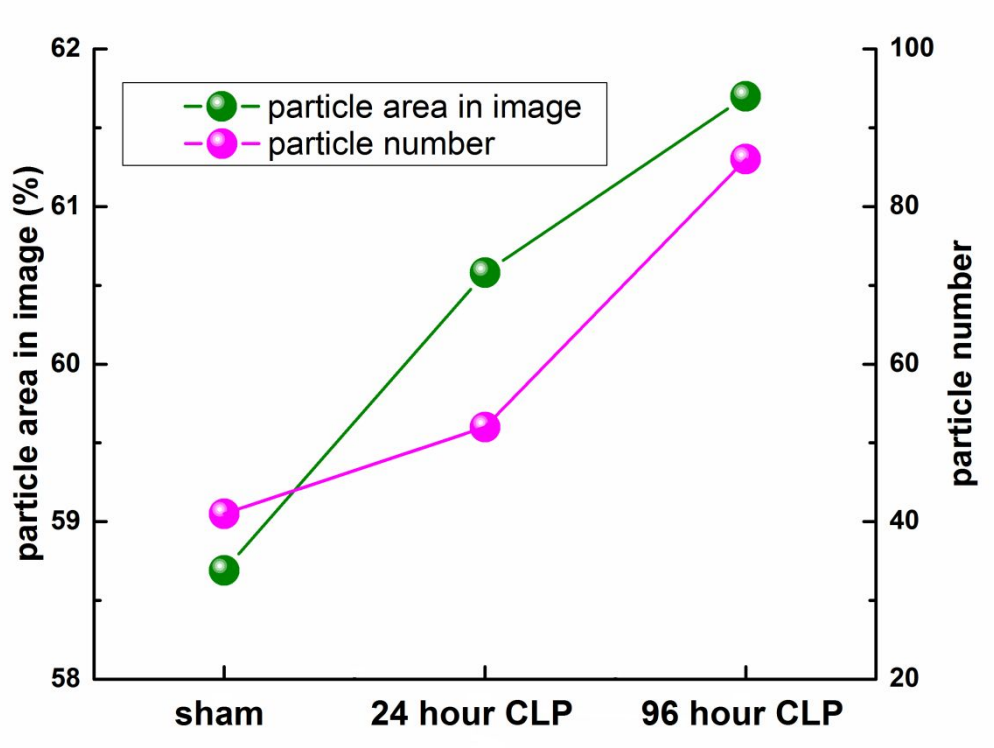

Figure S7. Mineral particle area and numbers of in-plane (x-y plane) particles determined from the AM-FM topography images of *sham*, *24 hour CLP* and *96 hour CLP* bone samples.

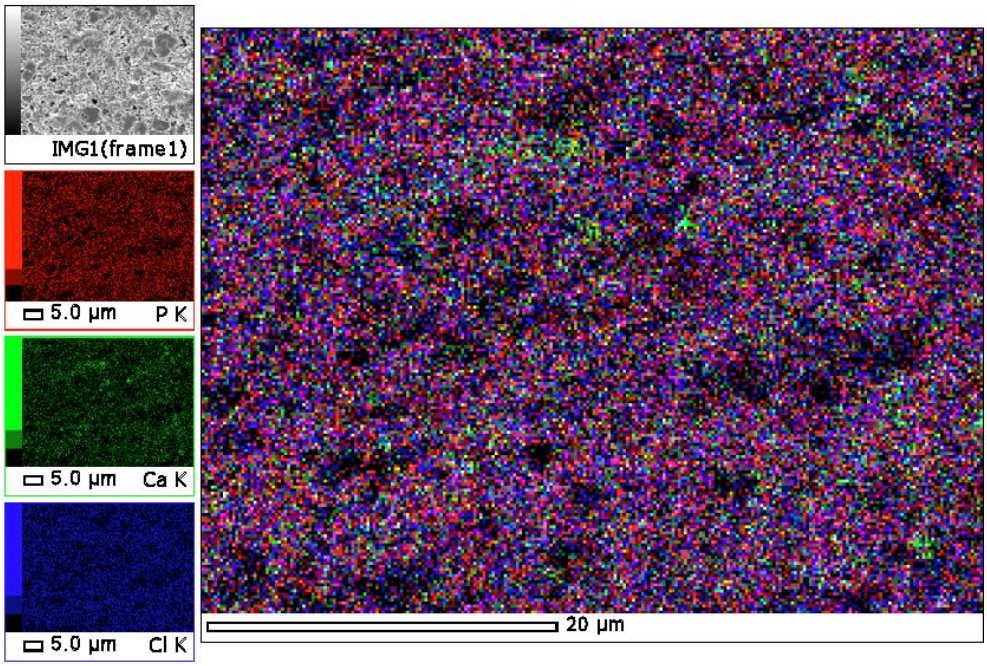

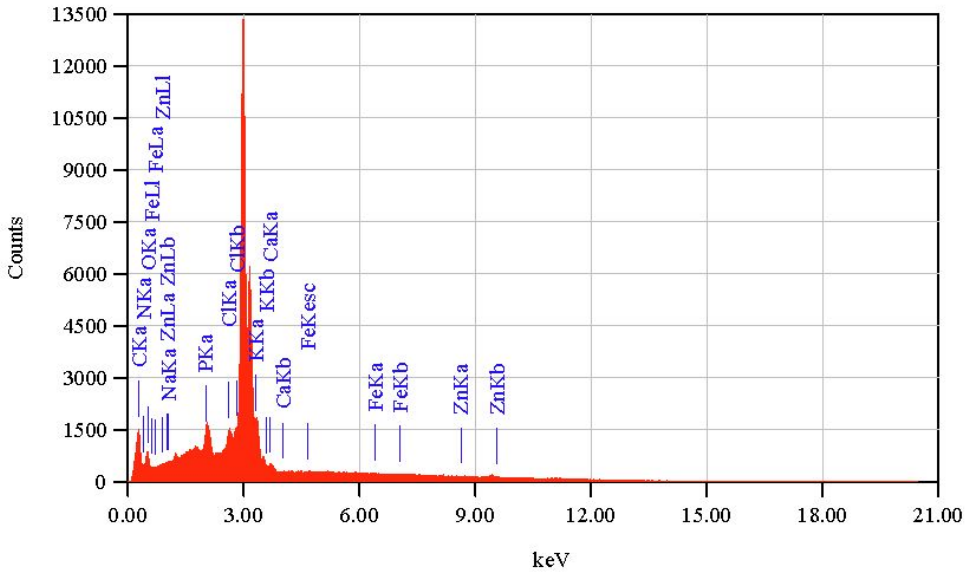

ZAF Method Standardless Quantitative Analysis
Fitting Coefficient : 0.9768

Element	(keV)	Mass%	Sigma	Atom%	Compound	Mass%	Cation	K
C K	0.277	51.88	0.38	64.24				30.4472
N K								
O K	0.525	31.24	0.64	29.04				37.8511
Na K								
P K	2.013	3.59	0.22	1.72				7.3293
Cl K	2.621	7.77	0.24	3.26				15.0712
K K								
Ca K	3.690	2.80	0.23	1.04				5.3047
Fe K	6.398	1.94	0.40	0.52				2.8957
Zn K	8.630	0.79	1.10	0.18				1.1008
Total		100.00		100.00				

Figure S8. Energy-dispersive X-ray spectroscopy (EDS) elemental images and quantitative chemical analysis of mineral from the *sham* bone sample.

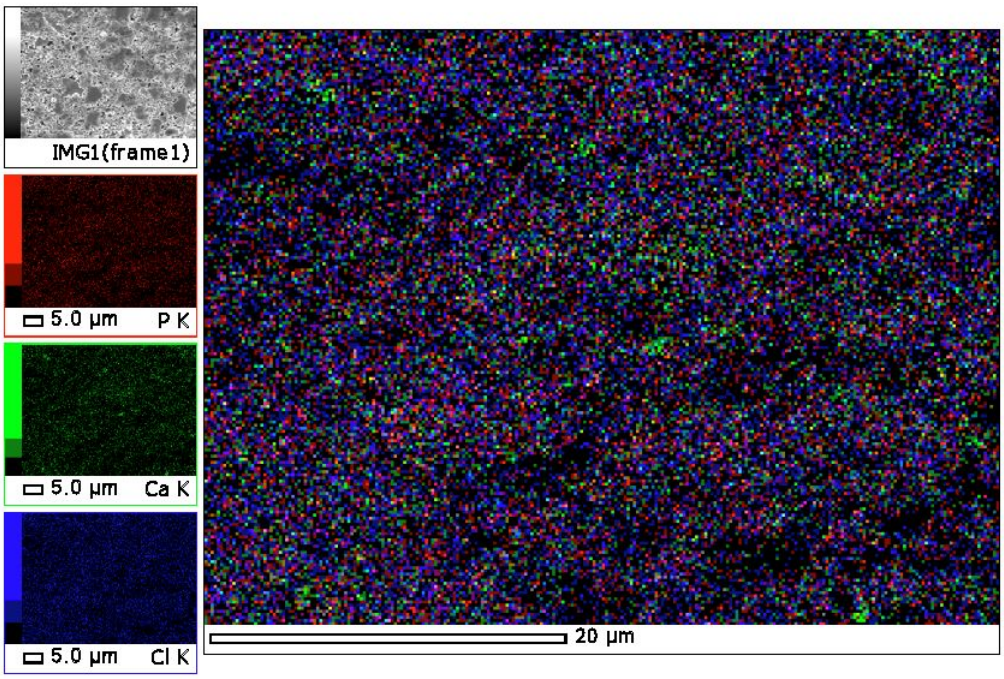

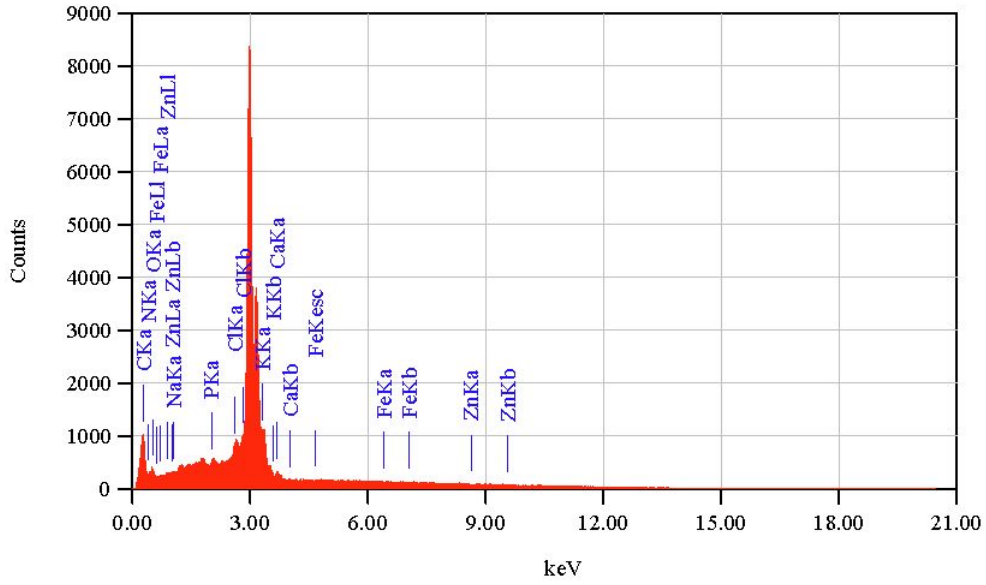

ZAF Method Standardless Quantitative Analysis
Fitting Coefficient : 0.9793

Element	(keV)	Mass%	Sigma	Atom%	Compound	Mass%	Cation	K
C K	0.277	58.98	0.52	70.52				41.7742
N K								
O K	0.525	26.00	0.96	23.34				28.2130
Na K	1.041	1.06	0.34	0.66				1.7249
P K	2.013	0.97	0.25	0.45				2.0792
Cl K	2.621	8.03	0.35	3.25				16.4504
K K								
Ca K	3.690	4.96	0.34	1.78				9.7583
Fe K								
Zn K								
Total		100.00		100.00				

Figure S9. Energy-dispersive X-ray spectroscopy (EDS) elemental images and quantitative chemical analysis of mineral from the *24 hour CLP* bone sample.

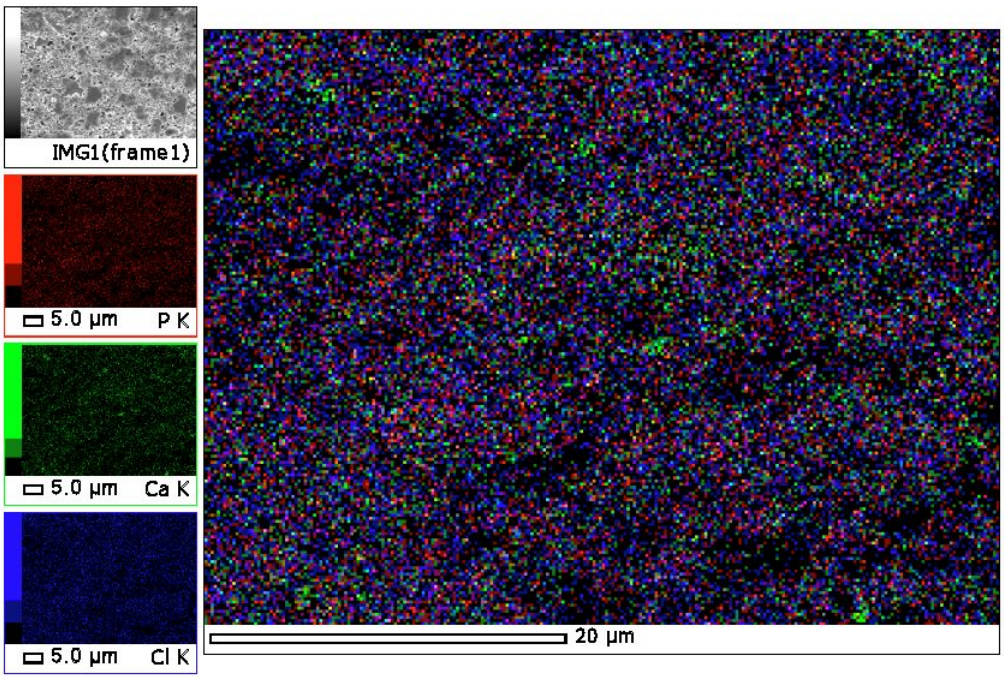

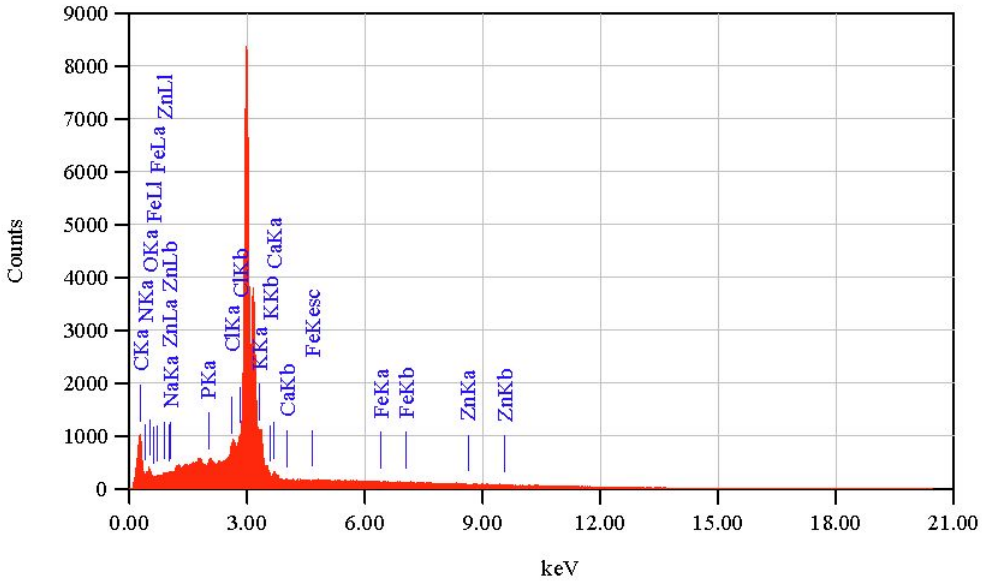

ZAF Method Standardless Quantitative Analysis
Fitting Coefficient : 0.9793

Element	(keV)	Mass%	Sigma	Atom%	Compound	Mass%	Cation	K
C K	0.277	58.98	0.52	70.52				41.7742
N K								
O K	0.525	26.00	0.96	23.34				28.2130
Na K	1.041	1.06	0.34	0.66				1.7249
P K	2.013	0.97	0.25	0.45				2.0792
Cl K	2.621	8.03	0.35	3.25				16.4504
K K								
Ca K	3.690	4.96	0.34	1.78				9.7583
Fe K								
Zn K								
Total		100.00		100.00				

Figure S10. Energy-dispersive X-ray spectroscopy (EDS) elemental images and quantitative chemical analysis of mineral from the *96 hour CLP* bone sample.

Table S1. Probe specification of AC200TS.

Specification	Values
First eigenmode resonant frequency, kHz	150
Second eigenmode resonant frequency, MHz	820
First eigenmode InvOLS,[a] nm/V	50.51
First eigenmode stiffness k, N/m	8~12
Cantilever dimension (L, W, H), μm	200, 40, 3.5
Tip radius of curvature, nm	8±2
Coating (tip and cantilever)	None

a) InvOLS: inverse optical lever sensitivity.

Table S2. Sample uncertainty analyses on collagen fibers and mineral from the *sham*, *24 hour CLP* and *96 hour CLP* bone samples based on 40 F-Z curves with 95% CI respectively.

Variable (x)	Description	Sample		Value (—)	Stand uncertainty (u_x) (—)	Sensitivity ($\frac{dE}{dx}$) (GPa)	Variance Contribution ($(\frac{dE}{dx}du_x)^2$) (GPa^2)
m	**Nondimensional photodiode sensitivity**	*Sham*	Collagen	0.0293	0.0006	6.9721	1.79e-5
			Mineral	0.0774	0.0095	7.7258	0.0054
		24 hour	Collagen	0.0779	0.0039	0.2893	1.3e-6
		CLP	Mineral	0.1106	0.0105	5.7604	0.0037
		96 hour	Collagen	0.1258	0.0057	0.6521	1.39e-5
		CLP	Mineral	0.1159	0.0041	8.9153	0.0013
						Expanded uncertainty (k_p=2) (GPa)	**Variance** (GPa^2)
E	**Elastic modulus**	*Sham*	Collagen	6.22	1.4472	2.8945	2.0945
			Mineral	106	25.132	50.263	631.60
		24 hour	Collagen	1.56	0.6425	1.2849	0.4128
		CLP	Mineral	102	36.019	72.037	1297.3
		96 hour	Collagen	5.35	2.0983	4.1966	4.4028
		CLP	Mineral	57.4	20.176	40.353	407.08

Table S3. Probe specification of AC160TS.

Specification	Values
First eigenmode resonant frequency, kHz	300
Second eigenmode resonant frequency, MHz	1.67
First eigenmode InvOLS,[a] nm/V	54.93
First eigenmode stiffness k, N/m	33~39
Cantilever dimension (L, W, H), μm	160, 40, 3.7
Tip radius of curvature, nm	8±2
Coating (tip and cantilever)	None

b) InvOLS: inverse optical lever sensitivity.

References

1. Sun, Y.; Hu, Z.; Zhao, D.; Zeng, K. Mechanical Properties of Microcrystalline Metal–Organic Frameworks (MOFs) Measured by Bimodal Amplitude Modulated-Frequency Modulated Atomic Force Microscopy. *ACS Appl. Mater. Interfaces* **2017,** *9* (37), 32202-32210. DOI: 10.1021/acsami.7b06809.
2. Garcia, R. Amplitude Modulation Atomic Force Microscopy. In *WILEY-VCH Verlag GmbH&Co. KGaA, Weinheim*, 2010.
3. Ryan, W.; Robert, M.; Jon, P.; Gordon, S.; Arvind, R. Uncertainty Quantification in Nanomechanical Measurements Using the Atomic Force Microscope. *Nanotechnology* **2011,** *22* (45), 455703.
4. García, R.; San Paulo, A. Attractive and Repulsive Tip-Sample Interaction Regimes in Tapping-Mode Atomic Force Microscopy. *Phys. Rev. B* **1999,** *60* (7), 4961-4967. DOI: 10.1103/PhysRevB.60.4961.
5. Hamaker, H. C. The London—van der Waals Attraction Between Spherical Particles. *Physica* **1937,** *4* (10), 1058-1072. DOI: https://doi.org/10.1016/S0031-8914(37)80203-7.
6. Chia-Yun, L.; Sergio, S.; Matteo, C. Reconstruction of Height of Sub-Nanometer Steps with Bimodal Atomic Force Microscopy. *Nanotechnology* **2016,** *27* (7), 075701.
7. Lai, C.-Y.; Perri, S.; Santos, S.; Garcia, R.; Chiesa, M. Rapid Quantitative Chemical Mapping of Surfaces with Sub-2 nm Resolution. *Nanoscale* **2016,** *8* (18), 9688-9694. DOI: 10.1039/C6NR00496B.